AJNR

Sonographic diagnosis of cisternal subarachnoid hemorrhage in the premature infant.

E Kazam, R Rudelli, W Monte, W A Rubenstein, E Ramirez de Arellano, R Kairam and N Paneth

Sonographic Diagnosis of Cisternal Subarachnoid Hemorrhage in the Premature Infant

Elias Kazam, Raoul Rudelli, William Monte, William A. Rubenstein, Elizabeth Ramirez de Arellano, Ram Kairam, and Nigel Paneth

PURPOSE: To evaluate sonographic criteria for the diagnosis of subarachnoid, and particularly cisternal, hemorrhage in the preterm infant. **METHODS:** The subarachnoid cisterns were studied on cadaveric anatomic sections and on postmortem ultrasonograms, as well as on in vivo ultrasonograms of healthy neonates. Based on the normal ultrasound appearances of these cisterns, criteria were developed for the recognition of abnormal cisternal fluid collections, which strongly suggest the presence of subarachnoid hemorrhage in the premature infant. These criteria were evaluated prospectively in a group of 63 preterm infants who underwent subsequent autopsy. **RESULTS:** In the 63 infants with neuropathologic verification, increased echogenicity and/or increased echo-free content of the subarachnoid cisterns correctly predicted subarachnoid hemorrhage with an accuracy of 75%, sensitivity of 69%, and specificity of 93%. The positive and negative predictive values were 97% and 46%, respectively. In 47% of the cases, ultrasound correctly detected cisternal subarachnoid hemorrhage before intraventricular hemorrhage could be diagnosed. **CONCLUSION:** A highly specific, although somewhat insensitive, sonographic diagnosis of subarachnoid hemorrhage can be made from the appearance of the subarachnoid cisterns. The diagnosis of subarachnoid hemorrhage may predate the ultrasound diagnosis of intraventricular hemorrhage and may alert the neonatologist to the need for follow-up sonograms in the absence of ultrasound evidence of intraventricular hemorrhage.

Index terms: Subarachnoid space, hemorrhage; Subarachnoid cisterns; Ultrasound, in infants and children; Infants, newborn

Several authors have commented on the difficulty of diagnosing subarachnoid hemorrhage with neonatal brain sonography (1–7). This difficulty has been attributed to the failure of subarachnoid blood to form a well-defined echogenic blood clot (5). Fresh liquified blood is rarely dis-

tinguishable from normal cerebrospinal fluid on ultrasound, but is readily detectable as a hyperdense area on computed tomography (CT) (1, 6). As a result, false-negative sonographic diagnoses of subarachnoid hemorrhage have been encountered frequently in comparative studies of ultrasound, CT, and autopsy findings (1–3). Prominence of the subarachnoid spaces is a common finding in premature infants (8) and has been found unreliable for the diagnosis of subarachnoid hemorrhage (2). Focal increased echogenicity and echo-poor widening of the sylvian fissures were reported to be 88% specific for detecting subarachnoid hemorrhage in a comparative study of ultrasound with CT and autopsy (9). However, the sensitivity of this sign was not assessed in that retrospective study (9). Furthermore, echo-poor widening of the sylvian fissures seemed to be a potential source of false-positive diagnoses (9). We have found the subarachnoid cisterns to be reliable sonographic indicators of abnormal
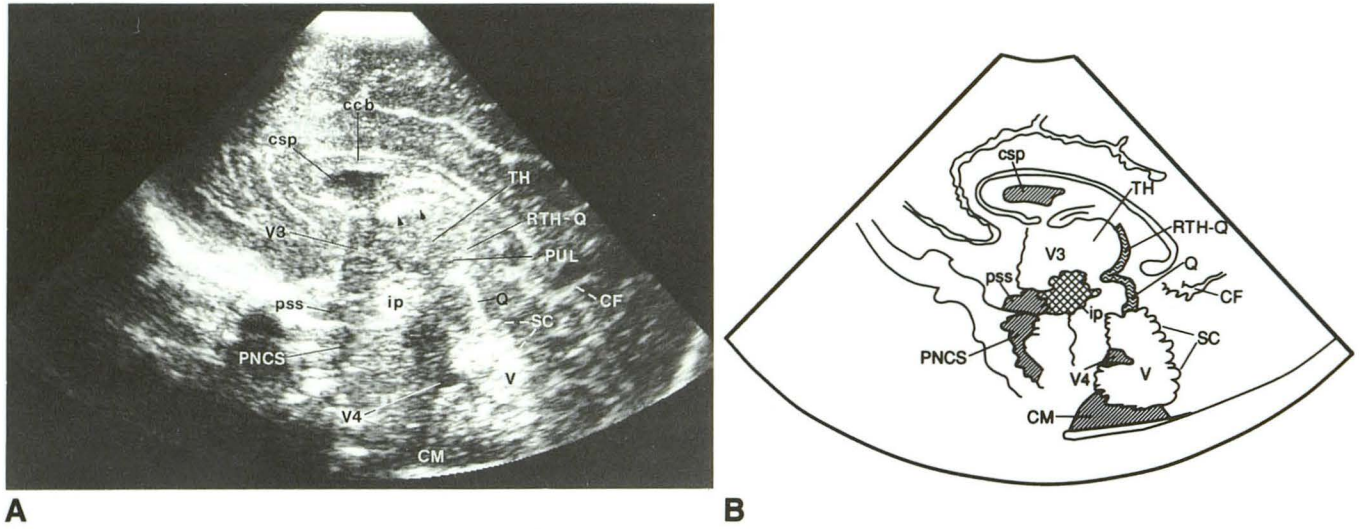
Fig. 1. *A*, Normal midsagittal sonogram and *B*, corresponding line drawing. The lower quadrigeminal cistern (*Q*) is visible as a homogeneously echogenic rind with short interlaced echo-poor lines, directly posterior to the echo-poor quadrigeminal plate. The retrothalamic cistern, which actually lies on either side of the midline, may be seen because of volume averaging as a curvilinear echogenic interface, again with an interlaced echo-poor–echogenic linear pattern, indistinguishable from the upper quadrigeminal cistern (*RTH-Q*). Echogenic choroid plexus (*small arrowheads*) attached to the roof of the third ventricle (*V3*). The calcarine fissure (*CF*) lies directly behind the quadrigeminal cistern. The echogenic superior cerebellar cistern (*SC*) is contiguous to the echogenic vermis (*V*), from which it is not normally separable. The cisterna magna (*CM*) is echo-poor in the midline, as is the posterior suprasellar cistern (*pss*), which lies directly anterior to the echogenic interpeduncular cistern (*ip*). The pontine cistern (*PNCS*) appears as an echo-poor stripe, directly anterior to the echogenic ventral pons. *TH* indicates thalamus; *PUL*, pulvinar; *V4*, fourth ventricle; *csp*, cavum septi pellucidi; and *ccb*, body of corpus callosum.
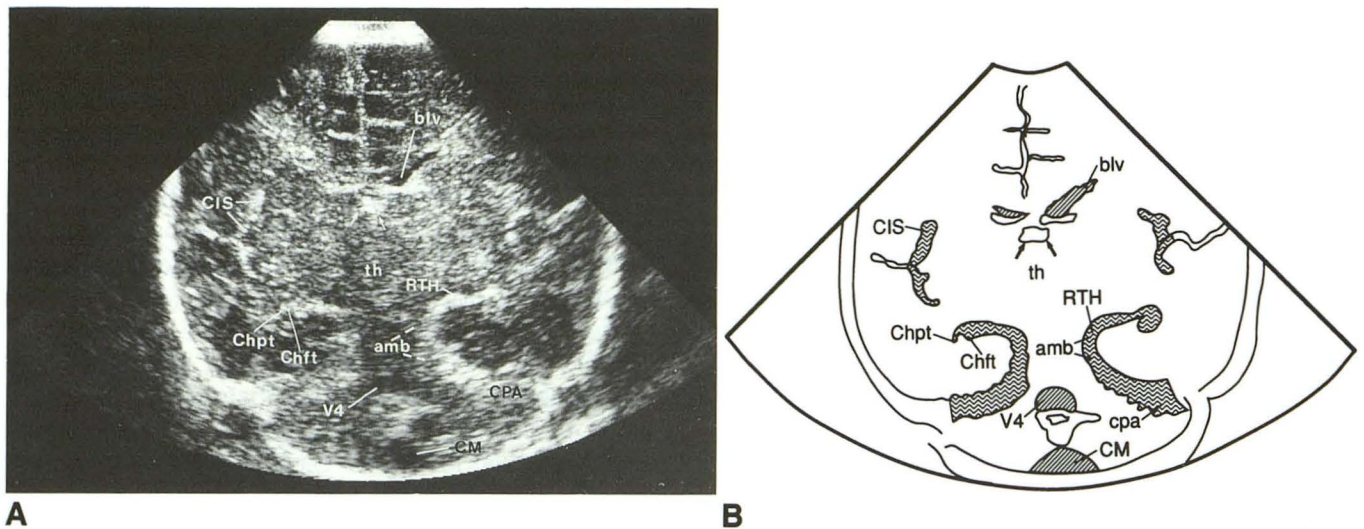

Fig. 2. *A*, Normal semicoronal sonogram and *B*, corresponding line drawing. The ambient cistern (*amb*), with its normal linear interlaced echogenic–echo-poor pattern, occupies the midportions of the echogenic C-shaped and reverse-C-shaped structures on either side of the echo-poor midbrain. The inferior limbs of the "C" represent the tentorium, which is not delineated, and the contiguous subtentorial and supratentorial subarachnoid space, continuous inferolaterally with the cerebellopontine angle cistern (*CPA*). The superior portions of the "C" represent the echogenic retrothalamic cisterns (*RTH*) and more laterally the choroid fissure (*Chft*) and attached choroid plexus (*Chpt*) of the temporal horn. There is a slightly distended left body of the lateral ventricle (*blv*). The echogenic circular sulcus (*CIS*), again with an interlaced linear pattern, overlies the echo-poor insula. *CM* indicates cisterna magna; *V4*, fourth ventricle; and *small arrows*, echogenic choroid plexus of the third ventricle.

subarachnoid, and especially *cisternal*, fluid collections. In this paper we describe our diagnostic criteria for such fluid collections and assess their clinical value as indicators of subarachnoid hemorrhage on sonography of the premature infant.

Methods

Research Plan and Subjects

The subarachnoid cisterns were studied on sonograms of three stillborn cadavers with gestational ages of 24 to 28 weeks, which were then sectioned in coronal or sagittal plains corresponding to the sonograms. The cisterns were also evaluated on sonograms of 56 healthy term infants (10) and 50 low-birth-weight (≤1500 g) infants. The normal appearances of these cisterns are illustrated in Figures 1 and 2 and summarized in Table 1. Based on the appear-

ances of the normal cisterns, criteria were developed for the ultrasound diagnosis of abnormal cisternal fluid collections (Table 1).

These criteria were then evaluated in a group of 63 preterm infants who underwent subsequent autopsy. The patients were subjects in a multicenter epidemiologic study of neonatal brain hemorrhage. The study included all very-low-birth-weight infants (501 to 2000 g) who were admitted to the intensive care units of three central New Jersey hospitals during a 34-month period, between August 27, 1984, and June 30, 1987 (11–13). Each study subject received a bedside cranial sonogram at approximately 4 hours, 24 hours, and 7 days after birth, unless precluded by early death. Additional sonograms were obtained when requested by the infants' physicians. Overall, 75 autopsies were performed as part of the multicenter study, but the ultrasound scans were available for only the 63 infants reported here. Postmortem sonograms were performed in

TABLE 1: Criteria for normal and abnormal cisternal echogenicity

| Cistern	Normal Sonography	Abnormal Sonography
Lower quadrigeminal (midsagittal ultrasonography, posterior to quadrigeminal plate)	a. Echogenic rind 1–3 mm, of *finely interlaced gracile echogenic and echopoor lines* (Figs 1, 3A, 8A) b. Echo-poor zone 1–3 mm, posterior to a, in larger infants or with high-resolution ultrasonography	a. *Hyperintense, confluent* echoes without interlacing (Figs 5A, 5B, 6A) b. Echo-poor zone >3 mm (Fig 7A) c. Increased mixed echogenic and echo-poor content (Figs 3B, 7B)
Upper quadrigeminal/retrothalamic (midsagittal ultrasonography)	1–3 mm rind of *finely interlaced* echoes, behind third ventricle or behind pulvinar (Figs 1, 3A)	Same criteria as for lower quadrigeminal cistern (a–c above) (Figs 5B, 6A, 7A)
Superior cerebellar		
Midsagittal ultrasonography	Indistinguishable from echogenic vermis (Figs 1, 3A)	Echo-poor and/or echogenic zone, contiguous to vermis (Figs 5A, 5B, 6A)
Semicoronal ultrasonography	Indistinguishable from vermis or supratentorial spaces (Fig 2)	Asymmetric increased or decreased echogenicity (Figs 3C, 3D)
Ambient (semicoronal ultrasonography)	a. Curvilinear echogenic rind 1–3 mm, of *finely interlaced* echoes, on either side of midbrain (Fig 2) b. Echo-poor zone 1–3 mm parallel to a, probably the tentorium (Fig 4A)	a. *Asymmetric* increased echogenicity with *hyperintense, confluent* echoes (Fig 4A)
Interpeduncular (midsagittal ultrasonography)	Echogenic zone anterior to midbrain (Figs 1, 3A)	Increased *hyperintense* echoes, or echo-poor focus (Fig 5B)
Posterior suprasellar (midsagittal ultrasonography)	Echo-poor zone anterior to echogenic interpeduncular cistern (Figs 1, 3A)	Echogenic focus (Fig 3B)
Cisterna magna		
Midsagittal ultrasonography	Echo-poor zone below vermis (Figs 1, 3A)	Echogenic focus (Fig 5A) or increased echo-poor content on consecutive sonograms
Semicoronal ultrasonography	Symmetrical echo-poor (Fig 2)	*Asymmetrical* echogenicity (Fig 3C)
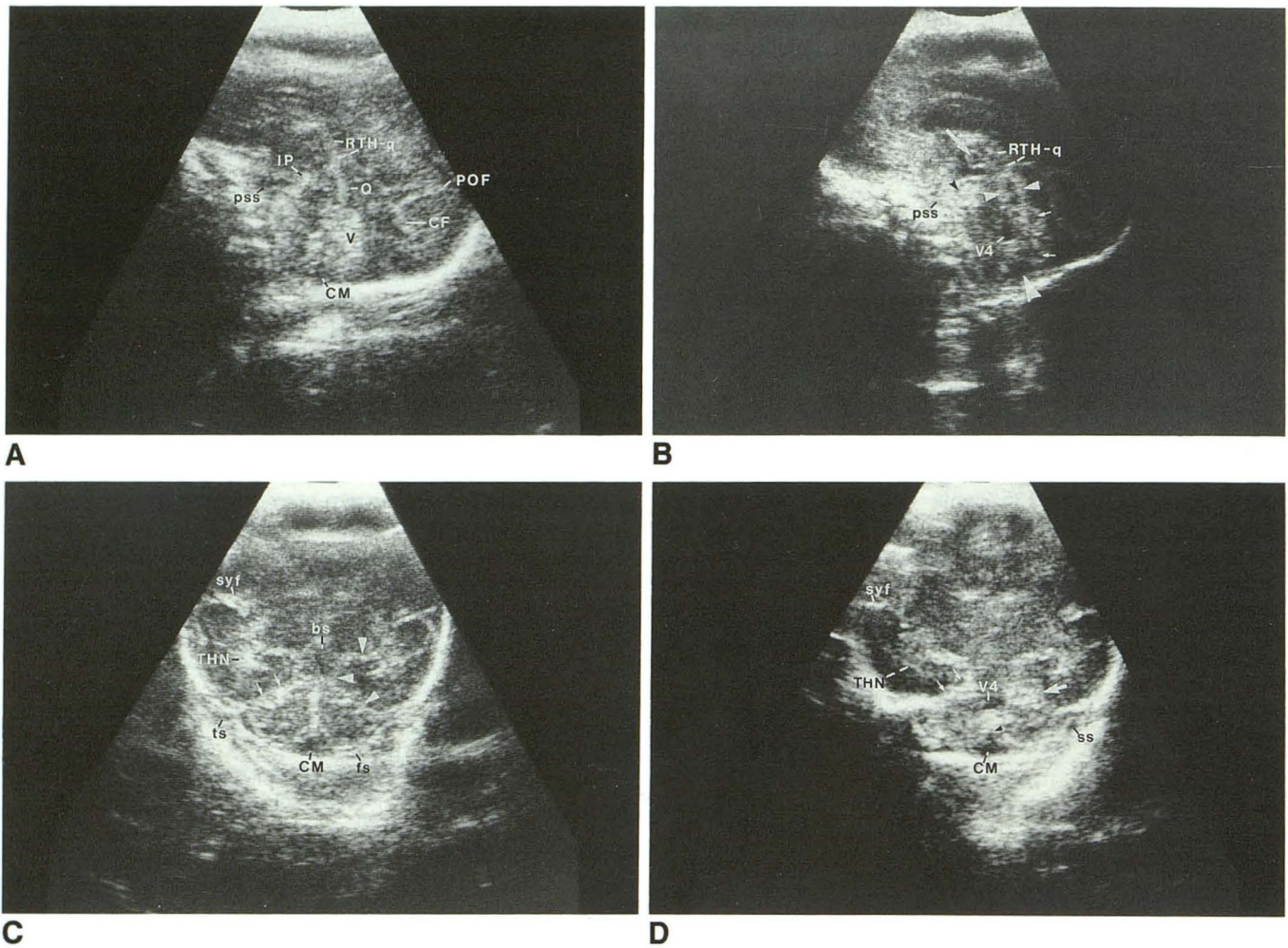
Fig. 3. Subarachnoid hemorrhage within the quadrigeminal, superior cerebellar, ambient, interpeduncular, posterior suprasellar, and great cisterns. Correlation of subtentorial subarachnoid hemorrhage with neuropathology.

A, Midline sagittal sonogram in a 4-hour-old, 973-g infant. The lower quadrigeminal cistern (*Q*), the junction of the retrothalamic and upper quadrigeminal cisterns (*RTH-q*), and the interpeduncular (*IP*) cistern have normal echogenicity, as do the parietooccipital (*POF*) and posterior calcarine (*CF*) fissures. The posterior suprasellar cistern (*pss*) is normally echo-poor. The slightly increased echogenicity within the cisterna magna (*CM*) may be artifactual and is not diagnostic of exudative cisternal fluid, such as cisternal blood. *V* indicates vermis.

B, Midline sagittal sonogram 16 days after A. The lower quadrigeminal cistern (*white arrowheads*) now has mixed echogenicity, with a relatively thick, irregular echogenic rind surrounding an echo-poor central portion, consistent with liquified subarachnoid blood clot (compare with A). A similar pattern is now evident more superiorly at the junction of the retrothalamic and upper quadrigeminal cisterns (*RTH-q*). Focal echo-poor areas (*small arrows*) suggest liquified blood clot within the superior cerebellar cistern and/or vermian fissures. Increased size and intensity of the confluent echoes within the interpeduncular cistern (*black arrowhead*), and loss of the normal echo-poor zone within the posterior suprasellar cistern (*pss*), are attributable to cisternal blood clot (compare with A). Partially liquified echogenic blood clot (*large arrow*) is now evident within a mildly dilated third ventricle. The fourth ventricle (*V4*) is also mildly dilated, when compared with A. The upper cisterna magna (*largest white arrowhead*) is now more distended, possibly with liquified hemorrhage.

C, Semicoronal sonogram at 4 hours obtained at the same time as A. A focus of asymmetrically increased echogenicity (*small

13 cases, but only 7 of these were available for this particular analysis.

Mean birth weight of the 63 infants was 934 g (±SD, 331) and ranged from 540 to 1660 g. Mean gestational age was 27.5 weeks (±SD, 3.3) and ranged from 22 to 38 weeks. Age at death ranged from 0.083 to 148 days with a mean of 11.7 days (±SD, 25). The interval from the last ultrasound to death ranged from 0.021 to 50 days, with a mean of 3.2 days (±SD, 7.3) and a median of 0.83 days.

Sonographic Methods

The sonograms were performed by hospital-based ultrasound technologists trained in the study protocol. At least 6, and usually 12 to 18, views were obtained with 5-, 6-, and/or 7.5-MHz transducers. The minimal coronal or semicoronal views required for each scan were at the anterior limits of the frontal horns, through the foramen of Monro, and at the trigones of the lateral ventricles. The minimal sagittal or parasagittal views required were in the midline and through the long axis of each lateral ventricle.

All sonograms in the group with neuropathologic verification had been reviewed previously by board-certified radiologists at the participating hospitals and by consultants to the study group. To assess the subarachnoid cisterns, the sonograms were reinterpreted by one of us, without knowledge of the other interpretations or of the neuropathologic findings.

Subarachnoid hemorrhage was diagnosed on the basis of increased echogenic or echo-poor content within the quadrigeminal, retrothalamic, superior cerebellar, ambient, interpeduncular, posterior, suprasellar, and great (magna) cisterns (Table 1 and Figs 3–8). The importance of true midline sagittal views and symmetrical semicoronal sonograms cannot be sufficiently emphasized, because obliquely oriented scans may lead to exaggeration of normal cisternal echogenicity. For the paired ambient cisterns, and for the cisterna magna which straddles the midline,

only *focal* and/or *asymmetrically* increased or decreased echogenicity was diagnostic of subarachnoid hemorrhage.

The fissures and the spaces over the convexities were not used for the diagnosis of subarachnoid hemorrhage in this study. Nevertheless, focal or diffusely increased echogenicity or echopenia of these spaces were recorded routinely for possible correlation with neuropathology. Particular attention was given to the sylvian, calcarine, and parietooccipital fissures which, unlike the spaces over the upper cerebral convexities, lie within the focal zone of the transducer and can be more reliably assessed for focal abnormalities.

Neuropathologic Methods

Brains were removed at the participating hospitals using a procedure described by Rudelli (Rudelli R, unpublished data). The cerebrum was sectioned initially along the three main coronal planes which corresponded to the ultrasound images. The resultant four cerebral blocks were then embedded totally in paraffin and sectioned serially at 10- to 50-micron intervals. Approximately 100 whole-brain sections (slides) per subject were examined. The brain stem and cerebellum were sectioned transversely. The cerebellum was further sectioned serially if cerebellar hemorrhage was suspected on gross examination. For each case, the presence and approximate location of subarachnoid hemorrhage were recorded, based on the gross examination and/or low-power magnification. Associated intraventricular hemorrhage, subependymal hemorrhage, ventricular dilation, and parenchymal abnormalities were also noted.

Results

Anatomic-Sonographic Correlations

The normal subarachnoid cisterns and sulci had a constant ultrasound appearance, without

---

arrows) is most consistent with blood in the right subtentorial space. Note the normal C-shaped configuration of the echogenicity (*arrowheads*) on the left side of the brain stem (*bs*). The inferior limb of the "C" (*lower arrowhead*) represents the tentorium (not visible separately) and the adjacent subtentorial and supratentorial subarachnoid space. The vertical midportion of the "C" represents the ambient cistern (*middle arrowhead*). The superior limb of the "C" (*upper arrowhead*) represents the retrothalamic cistern and the choroid fissure of the temporal horn. Focal increased echogenicity within the right temporal horn (*THN*) suggests intraventricular blood clot, adherent to the temporal choroid plexus. Increased linear echogenicity within the right sylvian fissure (*syf*) is also consistent with subarachnoid hemorrhage. There is a subtle, increased echogenicity of the cisterna magna (*CM*), just to the left of the midline, consistent with, but not diagnostic of, exudative (bloody) cisternal fluid (see Fig 1A). Normal increased linear echogenicity at the periphery of the cisterna magna is attributable to fibrous septa (*fs*). *ts* indicates transverse sinus.

D, Semicoronal sonogram and E, corresponding line drawing obtained 2 days after C. A new large echogenic focus (*large arrow*) is consistent with blood clot in the left subtentorial subarachnoid space, at the junction of the left cerebellopontine angle and ambient cisterns. The smaller right-sided focus of echogenic blood (*small arrows*) is unchanged to slightly less prominent. The temporal horn (*THN*) of the right lateral ventricle and the right sylvian fissure (*syf*) now appear unremarkable, consistent with resorption of previously noted echogenic blood clot. Similarly, the central portion of the cisterna magna (*CM*) now appears more homogeneously echopoor. The fourth ventricle (*V4*) is slightly distended. *ss* indicates sigmoid sinus; *black arrowhead*, vallecula.

E, Transverse (horizontal) neuropathologic section corresponding to D obtained 8 days later. The large blood clot (*arrows*) corresponds to the echogenic focus noted within the left subtentorial space, at the junction of cerebellopontine angle and ambient cisterns in D, but is clearly larger now than it was in D. The blood clot within the fourth ventricle (*V4*) was not visible in D. P indicates pons; *DN*, dentate nucleus.
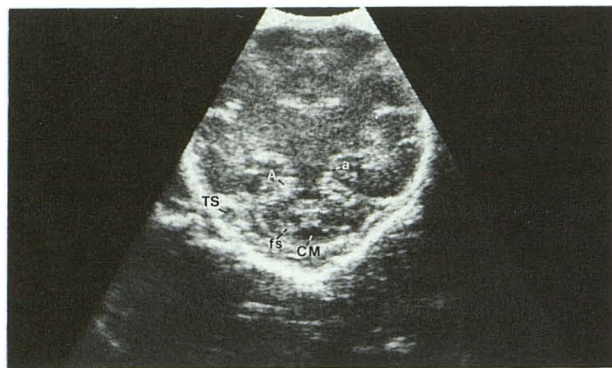
A
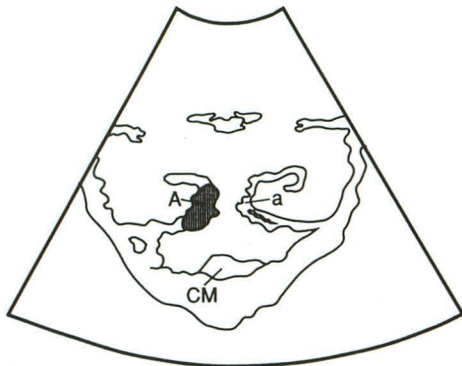
B
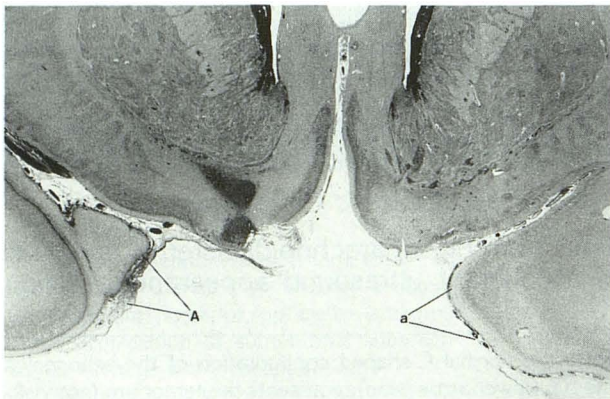
C

Fig. 4. Echogenic subarachnoid hemorrhage within the ambient cistern.

A, Semicoronal sonogram and B, corresponding line drawing in a 1-day-old infant with birth weight of 598 g. There is a focus of increased echogenicity in the right ambient cistern (A), consistent with cisternal blood clot, between the right temporal lobe and the midbrain. The curvilinear echo-poor zone in the left ambient cistern (a) is a normal finding and may represent the tentorium. The echo-free cisterna magna (CM) is normal. The linear echoes (fs) at the periphery of the cisterna magna are attributable to normal fibrous septa (see 3C). TS indicates transverse sinus.

B, Semicoronal neuropathologic section at the level of A obtained 14 days later. The brain stem and cerebellum have been removed. The blood clot (A) at the medial aspect of the right temporal lobe corresponds to the focal echogenicity noted within the right ambient cistern (A) in A. The left ambient cistern (a) is normal, as it was in vivo on the sonogram in A.

significant variations between the postmortem sonograms of the stillborn cadavers and the in vivo normal sonograms of the premature and term infants. In general the sulci and most cisterns were echogenic on ultrasound (Table 1 and Figs 1–8). The echogenicity was attributable to the small anteroposterior dimensions of these spaces and to the multiple acoustic interfaces created by blood vessels, and/or by fibrous arachnoid trabeculae which traversed the sulci and cisterns (14–18). The two cisterns that were consistently echo-poor (ie, the cisterna magna and the posterior suprasellar cistern) are anatomically deficient in arachnoid trabeculae and in blood vessels (Figs 1A, 2A, 3A, 3D, 4A, and 5A).

Abnormal cisternal echogenicity was not evident on the in vivo sonograms of the 50 premature infants with normal cranial sonograms. Among the 56 otherwise healthy term infants, the quadrigeminal cistern was found to be abnormal in two infants (4%): the echogenic rind exceeded 3 mm (6 and 8 mm) on midsagittal views, raising the possibility of subarachnoid hemorrhage. Neither term infant had other stigmata of intracranial hemorrhage, but both had had forceps delivery. There was no subsequent verification of the ultrasound findings.

Sonographic-Pathologic Correlations

Of the 63 cases with autopsy verification, there were 49 with subarachnoid hemorrhage and 14 without. Ultrasound correctly showed 34 of the positive and 13 of the negative cases. There were 15 false-negative and one false-positive ultrasound diagnoses of subarachnoid hemorrhage. The sonographic sensitivity for subarachnoid hemorrhage was 69% (34 of 49), with a specificity of 93% (13 of 14), and an overall accuracy of 75% (47 of 63). The positive and negative predictive values for the ultrasound diagnosis of subarachnoid hemorrhage were 97% (34 of 35) and 46% (13 of 28), respectively.

In 32 of the 34 cases (94%) with correct positive ultrasound readings of subarachnoid hemorrhage, there was exact correspondence between the sonographic and neuropathologic location of the blood clot in at least one cistern (Figs 3D, 3F, 4, 6A, 6C, 7B, and 7D). The two exceptions occurred in one case in which ultrasound showed subarachnoid hemorrhage within the quadrigeminal cistern, but pathologic examination revealed it to be within the contiguous superior cerebellar cistern, and in another case in which subarachnoid hemorrhage was diagnosed within the superior cerebellar cistern on ultrasound but was
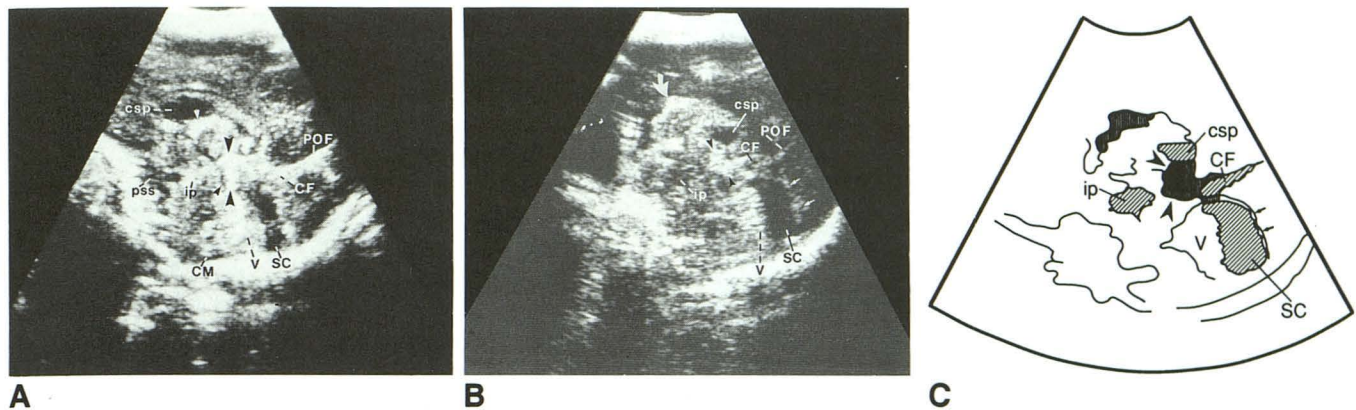
Fig. 5. Subarachnoid hemorrhage within the quadrigeminal, superior cerebellar, interpeduncular, and great cisterns. Extension of subarachnoid hemorrhage into the calcarine and parietooccipital fissures.

A, Midline sagittal sonogram in a 4-hour-old, 1080-g infant. A high-intensity echogenic rind (*large black arrowheads*), posterior to the aqueduct of Sylvius (*small black arrowhead*), is consistent with echogenic blood clot within the quadrigeminal cistern; compare with the normal appearance of this cistern in Figures 1A and 3A. The anterior calcarine (*CF*) and the parietooccipital (*POF*) fissures contain abnormally thickened high-intensity echoes consistent with subarachnoid hemorrhage; compare with the normal parietooccipital and calcarine fissures in Figures 1A and 3A. The curvilinear echopoor zone (*SC*), posterior to the vermis (*V*) is attributable to liquified blood clot within the superior cerebellar cistern. The linear echogenicity (*white arrowhead*), below the cavum septi pellucidi (*csp*), represents the choroid plexus in the roof of the third ventricle. Note the normally echogenic interpeduncular cistern (*ip*) and the contiguous, normally echo-poor, posterior suprasellar cistern (*pss*). High-intensity echoes within the cisterna magna (*cm*) are consistent with echogenic blood clot. Compare with Figures 1A, 3A–B.

B, Nearly midsagittal sonogram and C, corresponding line drawing obtained 1 day after A. Abnormally intense, confluent echoes are again seen in the quadrigeminal cistern (*black arrowheads*), consistent with subarachnoid hemorrhage. A large blood clot was noted in this same location at autopsy one day later. The previously echogenic focus (A) within the calcarine fissure (*CF*) is now echo-poor centrally (B), suggesting partial liquefaction of blood clot. The parietooccipital fissure (*POF*) now appears normal, suggesting interval resorption of echogenic blood clot. There has been a further increase in the anteroposterior dimension of the echopoor fluid in the superior cerebellar cistern (*SC*), with more posterior bowing of the posterior calcarine fissure (*small white arrows*). Increased echogenicity (*curved arrow*) at the anterosuperior aspect of the cavum septi pellucidi (*csp*) is attributable to blood clot within the adjacent lateral ventricular body and/or third ventricular roof. The previously echogenic interpeduncular cistern (*ip*) is now abnormally echopoor, suggesting liquified blood within this cistern. This was verified at autopsy. *V* indicates vermis.

seen only in the medullary cistern at autopsy. In general, subarachnoid hemorrhage was more extensive at autopsy than on ultrasound; thin layers of blood, which were easily visible on gross examination or on low power magnification, were not seen with ultrasound.

Among the 34 cases with correct positive ultrasound diagnoses of subarachnoid hemorrhage, the quadrigeminal, superior cerebellar, and ambient cisterns were the most frequently abnormal. Thus the quadrigeminal cistern was abnormal in 24 of 34 (73%) cases, mostly with increased echogenicity, or a mixed echogenic–echo-poor pattern. The superior cerebellar cistern was abnormal in 25 of 34 cases (74%), mostly with increased echo-poor content. The ambient cistern was abnormal in 11 of 34 cases (33%), with asymmetric increased echogenicity or a mixed pattern in most positive cases. Many cases had ultrasound abnormalities in more than one cistern. An evolving or changing pattern of cisternal echogenicity, attributable to clot retraction or liquefaction, was observed on consecutive sono-

grams in 15 of 34 (44%) cases. The only false-positive ultrasound diagnosis of subarachnoid hemorrhage resulted from a misinterpretation of upper quadrigeminal cistern echogenicity (Fig 8).

Focal increased or mixed echogenicity within the sylvian, calcarine, and parietooccipital fissures was observed in 5 of 34 cases (15%) with correct positive ultrasound diagnoses of subarachnoid hemorrhage. Increased subarachnoid echo-free fluid over the convexities, without associated echogenic foci, occurred in 38% of the 34 cases with correct positive ultrasound diagnoses, and in 37% (18 of 49) of all cases with subarachnoid hemorrhage at autopsy, but was also seen on ultrasound in 29% (4 of 14) of the cases without subarachnoid hemorrhage at autopsy—making it a relatively insensitive and nonspecific sign of subarachnoid hemorrhage.

Among the 15 false-negative cases, subarachnoid hemorrhage was found at autopsy within the quadrigeminal or superior cerebellar cisterns in 7 (47%), in the chiasmatic cistern in 3 (20%), and in the cisterna magna in 1 (6%). In the
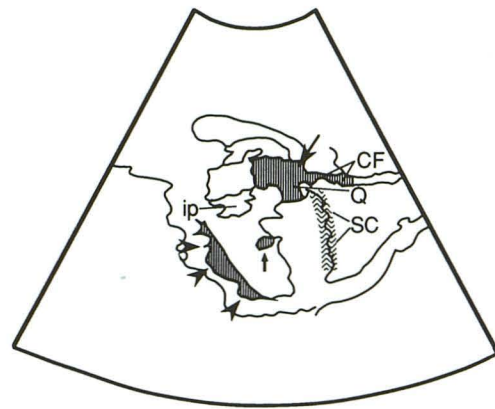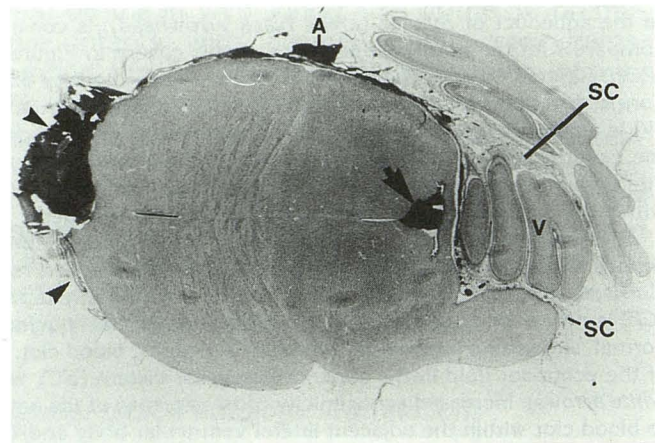
A

B

Fig. 6. Subarachnoid hemorrhage within the retrothalamic, upper quadrigeminal and superior cerebellar cisterns. Sonographic–pathologic correlation.

A, Midline sagittal sonogram and *B*, corresponding line drawing in a 15-day-old premature infant with birth weight of 666 g. There is increased focal echogenicity in the retrothalamic/upper quadrigeminal cisterns (*large arrow*), with extension into the anterior calcarine fissure (*CF*). The lower quadrigeminal (*Q*) and superior cerebellar (*SC*) cisterns are also abnormally echogenic, indicating cisternal blood clot. Note the loss of the normally convex contour of the vermis, caused by contiguous echogenic subarachnoid hemorrhage within the superior cerebellar cistern (compare with Figs 1A, 3A). The interpeduncular cistern (*ip*) appears unremarkable, but increased, heterogenous echogenicity in the pontine and medullary cisterns (*arrowheads*) is suggestive of subarachnoid hemorrhage. Compare with the normal appearance of these cisterns in Figures 1A and 3A. The fourth ventricle (*small arrow*) is not clearly demarcated because of

C

increased echogenicity of its contents, consistent with intraventricular hemorrhage. The *dotted line* marks the approximate level of the neuropathologic section obtained subsequently (Fig 6C).

C, Transverse (horizontal) neuropathologic section obtained 10 days after A at the approximate level shown by the dotted line in A. A resorbing, heterogeneous blood clot with hemolysis and partial liquifaction is visible within the superior cerebellar cistern (*SC*), around the vermis (*V*), corresponding to the increased echogenicity noted at the same location in A. Blood clot in a congealed, jellylike state, is also evident in *C* within the ambient (*A*) and pontine (*arrowheads*) cisterns, and in the fourth ventricle (*arrow*). Compare with A.

remaining 4 cases (27%), subarachnoid blood was found at autopsy only over the cerebral convexities or in the sylvian fissures, but not within the cisterns. Thus, there were only 11 false-negative sonograms for *cisternal* blood. As a result the sensitivity, specificity, and accuracy of the ultrasound diagnosis for *cisternal* subarachnoid hemorrhage were 76% (34 of 35), 94% (17 of 18), and 81% (51 of 63), respectively. The positive and negative predictive values for the diagnosis of *cisternal* subarachnoid hemorrhage were 97% and 61%, respectively (Table 2).

The ultrasound diagnosis of subarachnoid hemorrhage was apparently enhanced by the availability of multiple consecutive sonograms. For cases with two or more sonograms before autopsy, the diagnostic accuracy for subarachnoid hemorrhage was 85% (28 of 33), compared

with 63% (19 of 30) when only one sonogram was available (Table 2). The single false-positive diagnosis of subarachnoid hemorrhage occurred in an infant with only one sonogram (Fig 8).

The median and average intervals between the last sonogram and death were 0.8 and 3.3 days, respectively, for the group with correct sonographic diagnoses of subarachnoid hemorrhage, versus 1.0 and 3.1 days for the group with incorrect diagnoses. Postmortem sonograms were necessary for the correct positive ultrasound diagnosis of subarachnoid hemorrhage in three cases.

The accuracy of the ultrasound diagnosis of intraventricular hemorrhage in this study was 71% (45 of 63), with a sensitivity of 66% (33 of 50) and a specificity of 92% (12 of 13). The positive and negative predictive values for the
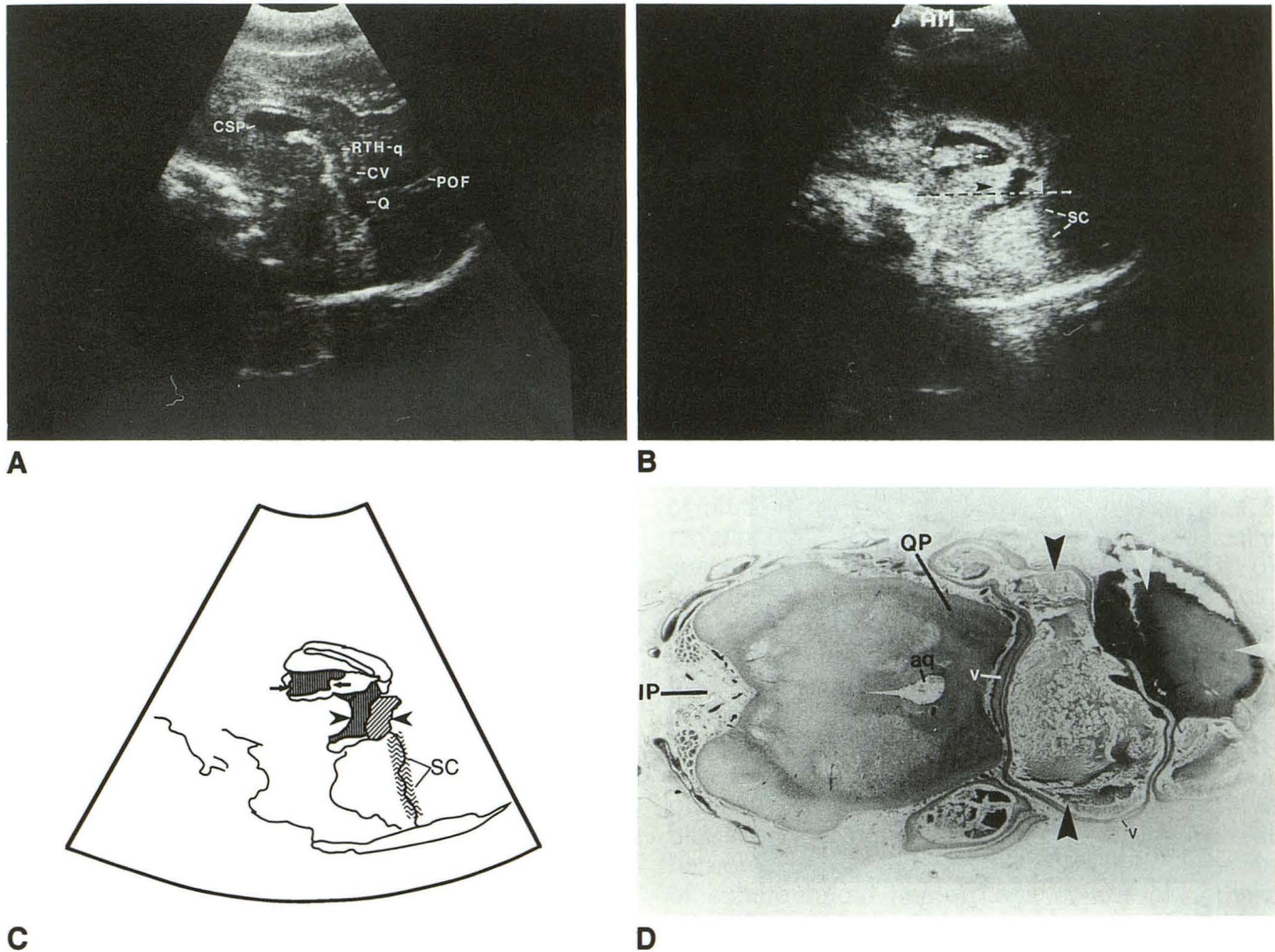
A

B

C

D

Fig. 7. Subarachnoid hemorrhage in the retrothalamic, velum interpositi, and quadrigeminal cisterns. Anatomic relationships to the cavum vergae and correlations with neuropathology.

A, Midline sagittal sonogram in a 4-hour-old, 1430-g infant. Echo-poor zones within the lower quadrigeminal (Q) and upper quadrigeminal-retrothalamic (RTH-q) cisterns are consistent with liquified subarachnoid blood clot. The cavum vergae (CV) lies posterior to, and is clearly demarcated from, the cisternal fluid. CSP indicates cavum septae pellucidi; POF, parietooccipital fissure.

B, Midsagittal sonogram and C, corresponding line drawing obtained 7 days after A. Echogenic and echo-free blood is evident within the retrothalamic-upper quadrigeminal cisterns (arrowheads). Echogenic intraventricular blood clot forms a fluid-blood level (arrows) within the dilated third ventricle. The normal posteriorly convex and anteriorly flat contour of the vermis has been replaced by an anteriorly convex intense echogenicity strongly suggestive of blood clot within the superior cerebellar cistern (SC) and vermian fissures. The dotted line marks the approximate level of the neuropathologic section obtained subsequently (D).

D, Transverse (horizontal) neuropathologic section through the brain stem obtained 7 days after A at the approximate level of the dotted line in B. There is a large blood clot (arrowheads) within the quadrigeminal cistern, posterior to the quadrigeminal plate (QP). The darker staining homogeneous portion of the blood clot (white arrowheads) corresponds to the echo-poor, jellylike portion of the cisternal hemorrhage in B. The lighter staining portion of the clot (black arrowheads) represents resorbing, heterogeneous blood clot within and around anteriorly displaced slivers of superior vermian tissue (V) and corresponds to the more echogenic component of the subarachnoid hemorrhage in B. IP indicates interpeduncular cistern; aq, aqueduct of Sylvius.

ultrasound diagnosis of intraventricular hemorrhage were 97% and 41%, respectively. Of the 34 cases with correct positive ultrasound diagnoses of subarachnoid hemorrhage, 33 also had intraventricular hemorrhage at autopsy, and 28 (85%) of these had correct positive sonographic diagnosis of intraventricular hemorrhage. In 16 of these 34 cases (47%), the initial ultrasound di-

agnosis of subarachnoid hemorrhage was made in the absence of positive ultrasound criteria for intraventricular hemorrhage.

There was a strong correlation between the pathologic findings of intraventricular hemorrhage and subarachnoid hemorrhage ($\chi^2 = 17.6$, $P < .001$). Both intraventricular hemorrhage and subarachnoid hemorrhage were present in 45
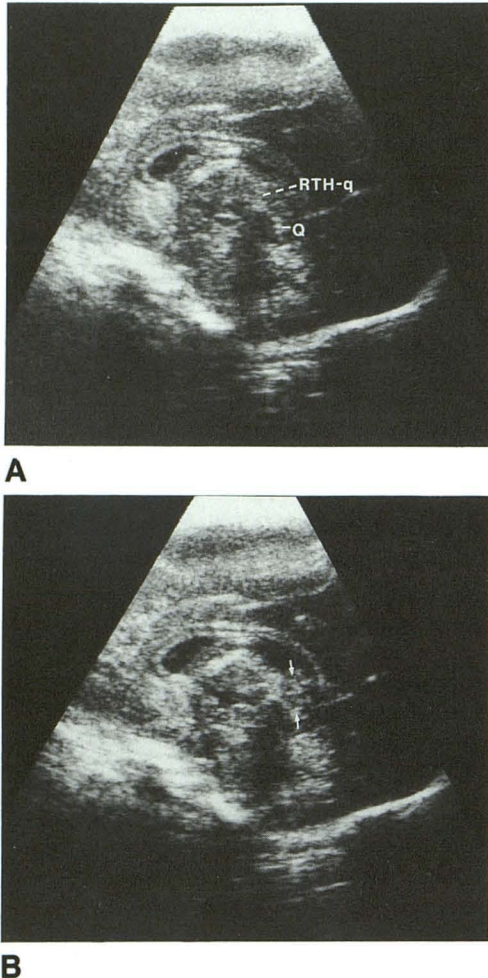
Fig. 8. The lower quadrigeminal cistern (Q) shows a normally thin curvilinear echogenicity in A, as does the junction of upper quadrigeminal and retrothalamic cisterns (RTH-q). However, increased echogenicity was suspected in the posterior aspect of these cisterns (arrows) in B. This led to a false-positive diagnosis of cisternal blood clot. In retrospect, the increased linear echoes in B are not confluent and show an interlaced pattern. They may have arisen, in part, from septa or septal veins in the posterior cavum septi pellucidi.

cases, and both were absent in nine cases. However, in 8% (5 of 63) of the cases, intraventricular hemorrhage was present in the absence of subarachnoid hemorrhage at autopsy; in four cases (6%), subarachnoid hemorrhage was found without intraventricular hemorrhage.

Discussion

In the first part of this study, which was based on anatomic sections and in vivo normal sonograms, the subarachnoid cisterns were found to have a constant sonographic appearance in premature and term infants, and on postmortem scans. In the second part of this study, which

was based on sonography of 63 infants with subsequent autopsy verification, increased echogenicity and/or echo-free content of the cisterns were shown to be highly *specific* but relatively insensitive criteria for the diagnosis of subarachnoid hemorrhage.

The ultrasound criteria for subarachnoid hemorrhage are not diagnostic of blood under all circumstances. Subarachnoid fluid collections, especially if echo-poor, may occur in infants with meningoencephalitis. Nevertheless, in the preterm infant, who is at high risk for intracranial hemorrhage, abnormal cisternal echogenicity is clearly a strong predictor of subarachnoid hemorrhage.

The sonograms for the pathologically proved cases were not intended originally to detect subarachnoid hemorrhage, and most were obtained without the high-resolution equipment currently available. Furthermore, CT correlation was not available in this series. These deficiencies are outweighed by the availability of meticulous autopsy verification, based on at least 100 whole-brain slides per subject. Routine midsagittal and coronal views were sufficient for detecting subarachnoid hemorrhage with high specificity (Figs 3–8).

Although the interval between the last sonogram and death was not ideal, it did not seem to affect the accuracy of the ultrasound diagnosis of subarachnoid hemorrhage, and it did not adversely influence the ultrasound–pathology comparisons, in view of the 94% correspondence between ultrasound and autopsy location of subarachnoid hemorrhage for at least one cistern per case (Figs 3D, 3F, 4A, 4C, 6A, 6C, 7B and 7D). This relatively good ultrasound–pathology correlation is attributable to the clotted, partially clotted, or jellylike consistency of most of the subarachnoid hemorrhage detected with ultrasound. The clots were visible either grossly or with low-power magnification at autopsy; higher-magnification microscopic views were not used to diagnose subarachnoid hemorrhage. Completely liquefied blood, without subsequent congealment, resorption, or organization of the clot, is unlikely to remain at the same location on autopsy, but is also more difficult to diagnose with ultrasound, on which it may mimic echo-free cerebrospinal fluid.

The quadrigeminal (Figs 3B, 5A, 5B, 6A, 6C, 7A and 7D), superior cerebellar (Figs 3B, 5A, 5B, 6A and 6C), and ambient (Figs 3D, 3F and 4) cisterns were the most important for the ultrasound diagnosis of subarachnoid hemorrhage. In fact, the correct ultrasound diagnosis of sub-

TABLE 2: Sonographic diagnosis of subarachnoid hemorrhage in 63 autopsy-proved cases

	1 All subarachnoid hemorrage* (n = 63)	2 All subarachnoid hemorrage* (US = 1†, n = 30)	3 All subarachnoid hemorrage* (US > 1‡, n = 33)	4 Cisternal subarachnoid hemorrage only (n = 63)
Sensitivity	69%	13/23 = 57%	21/26 = 81%	34/45 = 76%
Specificity	93%	6/7 = 86%	7/7 = 100%	17/18 = 94%
Positive predictive value	97%	13/14 = 93%	21/21 = 100%	34/35 = 97%
Negative predictive value	46%	6/16 = 38%	7/12 = 58%	17/28 = 61%
Overall accuracy	75%	19/30 = 63%	28/33 = 85%	51/63 = 81%

* Subarachnoid hemorrage in cisterns, fissures, and over convexities: columns 2 + 3.

† Cases with only one sonogram before autopsy.

‡ Cases with two or more sonograms before autopsy.

arachnoid hemorrhage depended solely on the midsagittal sonographic appearance of the quadrigeminal and superior cerebellar cisterns in 21% (7 of 34) of the cases. The upper quadrigeminal cistern was also the source of the only false-positive ultrasound diagnosis, because it appeared normal on one midsagittal view (Fig 8A) but was thought to be abnormally echogenic on another midsagittal image obtained during the same examination. In retrospect, the echoes that led to the false-positive diagnosis may have arisen from septal veins within the posterior cavum septi pellucidi or cavum Vergae.

Echogenic foci within the sylvian, calcarine, and parietooccipital fissures were diagnostic of subarachnoid hemorrhage, as was suggested in a previous report (9). However, this finding was noted in only a minority of the 34 cases with true positive ultrasound diagnosis of subarachnoid hemorrhage (5 of 34, 15%) and therefore constitutes a specific but insensitive sign of subarachnoid hemorrhage. In contrast, increased echo-free fluid over the cerebral convexities, without associated echogenic foci, was both insensitive and nonspecific for diagnosing subarachnoid hemorrhage. The torcular Herophili, the echo-free confluence of the dural sinuses above the cisterna magna (19), did not cause any diagnostic difficulties.

The accuracy and specificity of the ultrasound diagnosis of subarachnoid hemorrhage in this study compare favorably with previous reports (6, 7). The results are even better when the sonographic diagnosis of only *cisternal* hemorrhage is assessed (Table 2). In more than half of the false-negative sonograms (8 of 15), subarachnoid hemorrhage was found at autopsy within spaces not optimally positioned for ultrasound imaging. These include the spaces over the convexities, which lie in the near field of the transducer or at the lateral edges of the sound beam, and the basilar cisterns (eg, the chiasmatic, pon-

tine, and magna cisterns), which lie in the far field of the transducer, or in contiguity to the base of the skull. In view of the relatively low sensitivity of ultrasound for subarachnoid hemorrhage, CT remains a valuable method for detecting clinically suspected subarachnoid hemorrhage (1–3, 6) when sonography is negative.

The ultrasound diagnostic accuracy for intraventricular hemorrhage did not differ significantly from the accuracy for subarachnoid hemorrhage in this study. The results for intraventricular hemorrhage are also comparable to previously published reports (2, 20–23), after allowing for our preference of false-negative over false-positive ultrasound diagnoses. Although intraventricular hemorrhage was clearly the most common cause of subarachnoid hemorrhage at autopsy, there were discrepancies between these two diagnoses in 14% (9 of 63) of the cases. Thus the presence of intraventricular hemorrhage does not always imply subarachnoid hemorrhage, and vice versa. This fact highlights the advantage of correctly diagnosing both intraventricular hemorrhage and subarachnoid hemorrhage on sonography.

Nearly half (47%) of the initial correct positive ultrasound diagnoses of subarachnoid hemorrhage were made in the absence of positive criteria for intraventricular hemorrhage. In many of these cases, intraventricular hemorrhage became evident on subsequent sonograms. It is therefore likely that intraventricular hemorrhage was present on the initial ultrasound scan in these cases, either as echo-free blood blending imperceptibly with cerebrospinal fluid, or as echogenic blood obscured by contiguous choroid plexus. In such cases a sonogram positive for subarachnoid hemorrhage may alert the neonatologist to the possible presence of nondetectable intraventricular hemorrhage and therefore to the need for follow-up sonography.

The neurologic significance of subarachnoid hemorrhage in the premature infant is not clearly

defined. Subarachnoid hemorrhage predisposes to communicating hydrocephalus in the adult brain and may well have a similar effect in the neonate (6). Subarachnoid hemorrhage also causes cerebral vasospasm in adults (6, 24, 25) and may similarly contribute to cerebral ischemia in the neonate (26). Alternatively, subarachnoid hemorrhage may itself result from cerebral hypoxia (27).

In conclusion, a highly specific, although somewhat insensitive, sonographic diagnosis of subarachnoid hemorrhage can be made from the appearance of the subarachnoid cisterns on midline sagittal and semicoronal sonograms, obtained through the anterior fontanelle in low-birth-weight infants. The correct sonographic diagnosis of subarachnoid hemorrhage may precede the ultrasound diagnosis of intraventricular hemorrhage and may alert the neonatologist to the need for follow-up sonograms. Accurate sonographic detection of subarachnoid hemorrhage also may facilitate the future evaluation of the effects of subarachnoid hemorrhage on the neonatal brain.

Acknowledgments

References

1. Mack LA, Wright K, Hirsch JH, et al. Intracranial hemorrhage in premature infants: accuracy of sonographic evaluation. *AJR Am J Roentgenol* 1981;137:245–250

2. Babcock DS, Bove KE, Han BK. Intracranial hemorrhage in premature infants: sonographic-pathologic correlation. *AJNR Am J Neuroradiol* 1982;3:309–317

3. Thorburn RJ, Lipscomb AP, Reynolds EOR, et al. Accuracy of imaging of the brains of newborn infants by linear-array real-time ultrasound. *Early Hum Dev* 1982;6:31–46

4. Siegal MJ, Patel J, Gado MJ, Schackelford GD. Cranial computed tomography and real time sonography in full term neonates and in infants. *Radiology* 1983;149:111–116

5. Grant EG, Tessler F, Perrella R. Infant cranial sonography. *Radiol Clin North Am* 1988;26:1089–1110

6. Schellinger D. Comparison of two modalities: ultrasound versus computed tomography. In Grant EG, ed. *Neurosonography of the Pre-term Neonate.* New York: Springer-Verlag, 1986:94–111

7. Rumack CM, Johnson ML. Role of comput tomography and ultrasound in neonatal brain imaging. *J Comput Assist Tomogr* 1983;7:17–29

8. Lanman JT, Partanen Y, Ullberg S, Lind J. Extracortical cerebrospinal fluid in normal human fetuses. *Pediatrics* 1958;21:403–408

9. Ennis MG, Kaudi JV, Williams JL. Sonographic diagnosis of subarachnoid hemorrhage in premature newborn infants: a retrospective study with histopathologic and CT correlation. *J Ultrasound Med* 1985;4:183–187

10. Winchester P, Brill PW, Cooper R, Krauss AN, Peterson HdeC. Prevalence of "compressed" and asymmetric lateral ventricles in healthy full-term neonates: sonographic study. *AJNR Am J Neuroradiol* 1986;7:149–153

11. Pinto J, Paneth N, Kazam E, et al. Intraobserver variability in neonatal cranial ultrasonography. *Pediatr Perinatal Epidemiol* 1988;2:43–58

12. Pinto J, Paneth N, Kairam R, Rudelli R. Neuropathological validation of cranial ultrasound diagnosis in low birth weight infants: some preliminary observations. In: French J, Harel S, Casaer P, eds. *Child Neurology and Developmental Disabilities.* Baltimore: Brooks, 1988:185–190

13. Paneth N, Rudelli R, Monte W, et al. White matter necrosis in very low birth weight infants: neuropathologic and ultrasonographic findings in 22 infants surviving six days or more. *J Pediatr* 1990;116:975–984

14. Pernkopf E. *Atlas of Topographical and Applied Human Anatomy.* Vol 1, *Head and Neck.* Baltimore-Munich: Urban and Schwarzenberg, 1980:86–92

15. Wilson M. *The Anatomic Foundation of Neuroradiology of the Brain.* 2nd ed. Boston: Little Brown, 1972:113–146

16. Williams PL, Warwick R, eds. *Anatomy of the Human Body.* 36th ed. Philadelphia: Saunders, 1980:982–990,1049–1050

17. Yousefzadeh DK, Naidich TP. Ultrasound anatomy of the posterior fossa in children: correlation with brain sections. *Radiology* 1985;156:353–361

18. Naidich TP, Yousefzadeh DK, Gusnard DA. Sonography of the normal neonatal head: supratentorial structures: state-of-the-art imaging. In: Naidich TP, Quencer RM, eds. *Ultrasound of the Central Nervous System: Clinical Neurosonography.* Berlin-Heidelberg: 1980:30–49

19. Segal SR, Rosenberg HK. Sonographic appearance of the torcular Herophili. *AJNR Am J Neuroradiol* 1985;6:919–922

20. Kitchen WH, Ford GW, Murton LJ, et al. Mortality and two year outcome of infants of birthweight 500–1500 g: relationship with neonatal cerebral ultrasound data. *Aust Paediatr J* 1985;21:253–259

21. Grant EG, Borts FT, Schellinger D, McCullough DC, Sivasubramanian KN, Smith Y. Real-time ultrasonography of neonatal intraventricular hemorrhage and comparison with computed tomography. *Radiology* 1981;139:687–691

22. Pape KE, Bennett-Britton S, Szymonowicz W, Martin DJ, Fitz CR, Becker L. Diagnostic accuracy of neonatal brain imaging: a postmortem correiation of computed tomography and ultrasound scans. *J Pediatr* 1983;102:275–280

23. Hope PL, Gould SJ, Howard S, Hamilton PA, del Costello AM, Reynolds EOR. Precision of ultrasound diagnosis of pathologically verified lesions in the brains of very preterm infants. *Dev Med Child Neurol* 1988;30:457–471

24. Seiler RW, Grolimund P, Aaslid R, Huber P, Nornes H. Cerebral vasospasm evaluated by transcranial ultrasound correlated with clinical grade and CT-visualized subarachnoid hemorrhage. *J Neurosurg* 1986;64:594–600

25. Compton JS, Redmond S, Symon L. Cerebral blood velocity in subarachnoid hemorrhage: a transcranial Doppler study. *J Neurol Neurosurg Psychiatry* 1987;50:1499–1503

26. Volpe JJ, Herscovitch P, Perlman JM, Raichle ME. Positron emission tomography in the newborn: extensive impairment of regional cerebral blood flow with intraventricular hemorrhage and hemorrhagic intracerebral involvement. *Pediatrics* 1983;72:589–601

27. Towbin A. Central nervous system damage in the human fetus and newborn infant: mechanical and hypoxic injury incurred in the fetal neonatal-period. *Am J Dis Child* 1970;119:529–542